

Reversal of Solvent Migration in Poroelastic Folds

M. M. Flapper,¹ A. Pandey², M. H. Essink,¹ E. H. van Brummelen,³ S. Karpitschka⁴, and J. H. Snoeijer¹

¹*Physics of Fluids Group, Faculty of Science and Technology, Mesa+ Institute, University of Twente, 7500 AE Enschede, The Netherlands*

²*Department of Mechanical and Aerospace Engineering and BioInspired Syracuse, Syracuse University, Syracuse, New York 13244, USA*

³*Multiscale Engineering Fluid Dynamics Group, Department of Mechanical Engineering, Eindhoven University of Technology, P.O. Box 513, 5600 MB Eindhoven, The Netherlands*

⁴*Max Planck Institute for Dynamics and Self-Organization, 37077 Göttingen, Germany*

(Received 2 September 2022; accepted 4 April 2023; published 2 June 2023)

Polymer networks and biological tissues are often swollen by a solvent such that their properties emerge from a coupling between swelling and elastic stress. This poroelastic coupling becomes particularly intricate in wetting, adhesion, and creasing, for which sharp folds appear that can even lead to phase separation. Here, we resolve the singular nature of poroelastic surface folds and determine the solvent distribution in the vicinity of the fold tip. Surprisingly, two opposite scenarios emerge depending on the angle of the fold. In obtuse folds such as creases, it is found that the solvent is completely expelled near the crease tip, according to a nontrivial spatial distribution. For wetting ridges with acute fold angles, the solvent migration is reversed as compared to creasing, and the degree of swelling is maximal at the fold tip. We discuss how our poroelastic fold analysis offers an explanation for phase separation, fracture, and contact angle hysteresis.

DOI: 10.1103/PhysRevLett.130.228201

Polymer networks can absorb large amounts of solvents, driven by the entropy of mixing. The solvent migration in or out of an elastic network causes significant change in volume through swelling or shrinking [1]. This interplay between liquid transport and elasticity, known as poroelasticity, is intrinsic to a number of biophysical processes, e.g., bleb formation in cells [2] and skin maceration (hyperhydration) [3], and crucial for technological applications of soft materials such as “plasticizers” for softening “plastics” [4], hydro- and organogels in mechanobiology [5], or electronic encapsulants with self-healing properties [6].

The surfaces of soft poroelastic matter can exhibit sharp folds that can be either acute or obtuse. Obtuse poroelastic folds are found in creases, when swollen polymer networks spontaneously develop morphologies [7–9] where a surface folds onto itself [Fig. 1(a)]. These creases mimic the growth-induced gyrification of mammalian brains [10–12] and tumors [13]. Folds with acute angles are observed in wetting [14–17] and adhesion [18,19], where the substrate is pinched into an acute ridge of well-defined opening angle [Fig. 1(b)]. Both types of folds are expected to create a

divergence of elastic stress [20], but the implication of the fold geometry on the solvent distribution near the tip has barely been addressed [21,22]. Yet, the singular stress-solvent

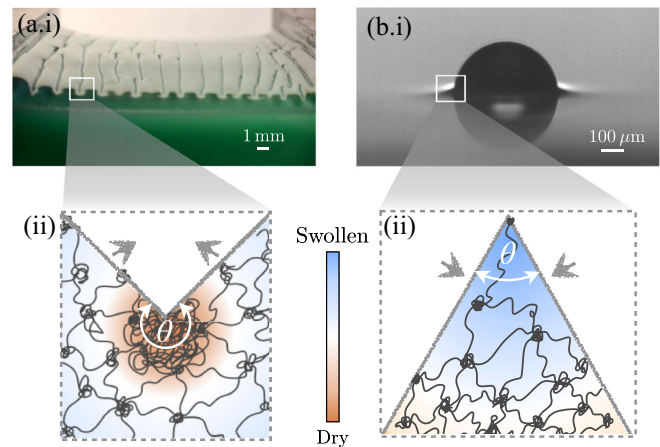


FIG. 1. Poroelastic folds in (a) creasing, with fold angles $\theta > \pi$, and (b) wetting, with $\theta < \pi$, leading to opposite solvent distributions. (a.i) Swollen or compressed surfaces can spontaneously fold into self-contacting creases. (a.ii) The obtuse fold gives rise to a blowup of pore pressure, squeezing out the solvent and causing a completely dry fold tip. A self-contacting crease corresponds to $\theta = 2\pi$. (b.i) A water drop on a soft PDMS gel, oblique side view. (b.ii) The acute fold angle at the wetting ridge causes a negative pore pressure, aspirating the solvent toward maximum swelling at the tip.

Published by the American Physical Society under the terms of the Creative Commons Attribution 4.0 International license. Further distribution of this work must maintain attribution to the author(s) and the published article's title, journal citation, and DOI. Open access publication funded by the Max Planck Society.

interaction will turn out to be central to unexplained observations such as the expulsion of solvent or uncross-linked chains [23–25], wetting induced fracture [26,27], and hysteretic phenomena in both wetting and creasing [28,29].

In this Letter we analyze the poroelastic fold singularity, resolving both the distribution of stress and the degree of swelling at equilibrium. We observe a reversal of solvent migration between “creasing” and “wetting,” by the mechanism described in Fig. 1. For creasing, the fold stretches the surface angle from $\theta = \pi$ (initially flat) to $\theta = 2\pi$; the polymer stress induced by this angular stretching generates a high pore pressure near the tip that “squeezes” the solvent out of the fold. The opposite trend is observed for wetting, where the surface angle is compressed to $\theta < \pi$, leading to a maximal aspiration of solvent toward the tip. We highlight how these intricate solvent distributions shed new light on recent experiments.

Poromechanics.—We start by considering a flat poroelastic substrate in the standard large-deformation framework [30], which deforms into a planar, two-dimensional fold. A solvent swells the elastic polymer network, characterized by a swelling ratio J that compares the swollen volume with that of the dry polymer network. Assuming both the solvent and polymer molecules to be incompressible, the polymer volume fraction naturally becomes $1/J$, while the liquid volume fraction ϕ is given by the remainder

$$\phi = 1 - 1/J. \quad (1)$$

This relates the dilation of the elastic network (J) to the volume fraction of the solvent (ϕ). Likewise, the free energy of a poroelastic material contains two contributions: a mixing energy that describes the interaction of the solvent with the polymers, and an elastic energy due to the stretching of the polymer network. The resulting stress tensor $\boldsymbol{\sigma} = -p\mathbf{I} + \boldsymbol{\sigma}_{\text{el}}$ consists of a pore (osmotic) pressure p and an elastic stress $\boldsymbol{\sigma}_{\text{el}}$. According to Flory-Huggins theory [31,32], the pore pressure at equilibrium reads

$$p(\phi) = -\frac{kT}{v} [\ln \phi + (1 - \phi) + (1 - \phi)^2 \chi] + \frac{\mu}{v}, \quad (2)$$

with v the volume per liquid molecule, χ the interaction parameter between solvent and network, and μ the solvent’s reference chemical potential. The pore pressure is a decreasing function of ϕ , and is always larger than the reference pressure $p(\phi = 1) = \mu/v$ of the pure solvent.

The other component of the stress tensor, the elastic stress $\boldsymbol{\sigma}_{\text{el}}$, is a function of the Finger tensor \mathbf{B} , which characterizes the stretching of the polymer network. The tensor is in general anisotropic, and the local volumetric swelling ratio follows from $J = \det(\mathbf{B})^{1/2}$. For long chain

polymer networks, a commonly used constitutive relation is the so called “neo-Hookean” model:

$$\boldsymbol{\sigma}_{\text{el}}(\mathbf{B}) = G(\mathbf{B} - \mathbf{I})/J, \quad (3)$$

where G is the shear modulus of the polymer network.

The degree of swelling prior to folding depends on the ratio of the osmotic pressure scale (kT/v), to the network’s elastic modulus (G). The latter can be expressed as $G = NkT$, where N represents the number of chains per unit volume [30]. With this, the problem is described by the dimensionless parameter $Nv = Gv/kT$. The preswelling volume fraction ϕ_0 of an isotropic medium, as described by the classical Flory-Rehner theory [33], is then recovered from $\boldsymbol{\sigma} = -\mu/v\mathbf{I}$. Typical values of ϕ_0 can be inferred from Fig. 2(a). We note that different hydrogels approximately cover the range $Nv = 10^{-4} \dots 10^{-1}$ [30], while a polymer network swollen with uncrosslinked chains has $Nv \sim 1$.

Fold geometry and mechanics.—The central aim is to resolve the stress singularity, which is manifestly anisotropic, and the resulting solvent distribution inside a fold. In polar coordinates, the most general, azimuthally symmetric fold is described by the mapping

$$\varphi = b\Phi, \quad r/\lambda(r) = R, \quad (4)$$

where (R, Φ) characterizes the material points of the substrate in the undeformed state [cf. Fig. 2(b)]. The first equation expresses how an azimuthal angle Φ in the reference state (prior to folding) is deformed into a new angle φ . We assume that this azimuthal deformation is uniform and defined by a factor $b = \theta/\pi$, where θ is the fold angle. The response in the radial direction is captured by the stretch, $\lambda(r)$, mapping the radial position of a point originally at R to the new position r . For incompressible media, volume conservation dictates $\lambda = b^{-1/2}$ [34]. However, poroelastic networks may swell: $\lambda(r)$ can grow well beyond the stretch for incompressible folds, and needs to be determined self-consistently. The Finger tensor \mathbf{B} corresponding to Eq. (4) reads (cf. Supplemental Material [35])

$$\mathbf{B} = \begin{pmatrix} \left(\frac{\lambda}{1-r\lambda'/\lambda}\right)^2 & 0 \\ 0 & (b\lambda)^2 \end{pmatrix} \underset{J \neq \infty}{\simeq} \begin{pmatrix} \lambda^2 & 0 \\ 0 & (b\lambda)^2 \end{pmatrix}. \quad (5)$$

In the second step it was assumed that J remains finite at the tip, in which case $|r\lambda'/\lambda| \ll 1$ [35]. With this, $J = b\lambda^2$, so that the local swelling ratio, and thus $p(\phi)$ can be expressed in terms of λ . The problem is closed by imposing mechanical equilibrium, $\nabla \cdot \boldsymbol{\sigma} = \mathbf{0}$, which owing to the azimuthal symmetry simplifies to

$$\frac{d\sigma_{rr}}{dr} = \frac{1}{r}(\sigma_{\varphi\varphi} - \sigma_{rr}). \quad (6)$$

This is a radial force balance that ultimately determines $\lambda(r)$, and thus the liquid fraction $\phi(r)$, near the tip.

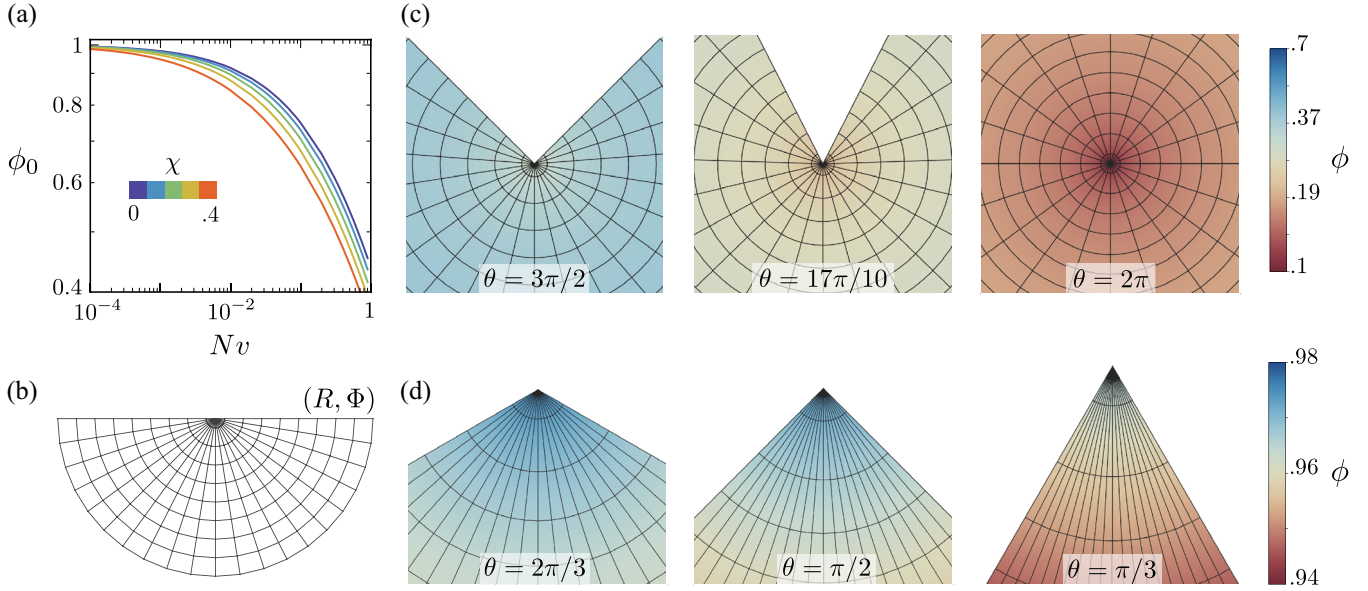


FIG. 2. Solvent migration into or out of poroelastic folds. (a) Preswelling volume fraction ϕ_0 as a function of Nv , for an unfolded substrate. (b) A polar grid (R, Φ) characterizes the material points in the unfolded substrate. (c),(d) Various folds for $Nv = 0.1$. The lines represent the deformed grid, folded to new positions (r, φ) . The color represents liquid volume fraction ϕ , which is enhanced or reduced with respect to the preswelling $\phi_0 \sim 0.8$. (c) Creasing: upward folds for increasing fold angle θ . A crease corresponds to $\theta = 2\pi$. The liquid fraction within a crease is given by Eq. (9). The dark red spot in the center indicates the dry-out near the crease tip. (d) Wetting: downward folds with decreasing fold angles. In contrast to creasing, swelling is strongly enhanced near the tip (dark blue). In this case, ϕ is given by Eq. (11), plotted for $I_{\max} = 100$.

Creasing.—Interestingly, it is crucial to distinguish creasing ($\theta = 2\pi$) from wetting ($\theta < \pi$), since the stress singularity takes on opposite signs. We first proceed for creasing, for which Eq. (5) gives the stress near the tip:

$$\sigma_{rr} = -\bar{p} + Gb^{-1}, \quad \sigma_{\varphi\varphi} = -\bar{p} + Gb. \quad (7)$$

Here, the isotropic part of σ_{el} is absorbed within the modified pressure $\bar{p} = p + G/J$. Using this stress to integrate the radial force balance, Eq. (6), gives the pressure

$$\bar{p}(r) = \bar{p}_0 - G(b - b^{-1}) \ln r/r_0. \quad (8)$$

The integration constant is conveniently expressed as a length scale r_0 , which represents the typical distance from the tip where we recover the pressure \bar{p}_0 in the bulk of the preswollen medium [38].

Having solved for the stress, we may determine the solvent distribution inside a poroelastic crease. For $b = \theta/\pi > 1$, the logarithmic divergence in Eq. (8) can indeed be generated by the pore pressure, Eq. (2). Namely, in the limit of $\phi \rightarrow 0$, one finds $\bar{p}(\phi) \simeq -(kT/v) \ln \phi$, so that

$$\phi = (r/r_0)^\beta, \quad \text{with } \beta = Nv(b - b^{-1}) > 0. \quad (9)$$

A central finding is thus that creasing induces an algebraic decay of the solvent fraction toward the fold tip. The exponent β is nontrivial, involving both the network properties Nv and the fold angle $b = \theta/\pi$. Noting that $\beta > 0$ for any angle $\theta > \pi$ implies that solvent is expelled

from the tip. Figure 2(c) shows this solvent distribution inside the fold for $Nv = 0.1$. Indeed, the volume fraction is everywhere below the preswelling bulk value ($\phi_0 \sim 0.8$). Most dramatically, the dark zone at the center indicates the complete dry-out of the crease tip.

Wetting.—Poroelastic wetting folds are fundamentally different in nature from creasing folds. Namely for $b < 1$, mechanical equilibrium, Eq. (8), requires a diverging negative pore pressure, aspirating liquid toward the fold tip. However, the lowest possible pressure that can be achieved is that of the pure solvent, μ/v , achieved for maximum swelling $\phi = 1$ or $J \rightarrow \infty$. This suggests a tendency toward “infinite swelling” for folds with $b < 1$, in which the polymer network is unphysically stretched, a paradox that was already anticipated from a small-deformation linear poroelastic calculation [21].

The infinite-swelling paradox can be resolved by accounting for strain stiffening of the polymer network. For large swelling, the polymers stretch to a degree that they can no longer be considered Hookean springs. This effect can be accounted for by an effective elastic modulus $\psi(I)G$, where $\psi(I)$ is an increasing function of the mean stretch $I = \text{tr}(\mathbf{B})$ [39]. We reanalyze the fold problem with $\sigma_{\text{el}} \simeq \psi \mathbf{GB}/J$, i.e., anticipating \bar{p} to become subdominant due to $\psi \gg 1$. Using Eq. (5) we then write $\sigma_{\varphi\varphi} = b^2 \sigma_{rr}$, so that integrating the radial force balance, Eq. (6), gives

$$\sigma_{rr} = (r_0/r)^{1-b^2} Gb^{-1}, \quad \Rightarrow \psi = (r_0/r)^{1-b^2}. \quad (10)$$

For $b < 1$, this gives a stress singularity that is now carried by the strain stiffening of the polymer network, rather than by the pore pressure. Specifically, the divergence of σ_{rr} implies that the polymers become maximally stretched at the tip.

Yet, the degree of swelling indeed remains finite within the standard framework for strain stiffening. For example in the Arruda-Boyce [40] or the Gent model [41,42], the function ψ diverges when I reaches its maximum extensibility I_{\max} , which indeed comes with a finite swelling ratio. For both the Arruda-Boyce and Gent model, the stress, Eq. (10), implies a volume fraction (cf. Supplemental Material [35]):

$$\phi \simeq 1 - \frac{b^{-1} + b}{I_{\max}} \left[1 + \left(\frac{r}{r_0} \right)^{1-b^2} \right]. \quad (11)$$

Strain stiffening, encoded via I_{\max} , thus offers a regular solution for $\theta < \pi$, with a finite ϕ at the ridge tip.

Figure 2(d) illustrates the strongly enhanced swelling within wetting ridges. The color map indicates that the solvent fraction is much larger than that of the preswollen medium ϕ_0 . From the circular gridlines, one also infers the very large stretching in the radial direction, which is bounded only by the finite extensibility of the polymers.

We validate this intricate wetting scenario using finite element simulations of a wetting ridge on a poroelastic layer of thickness H , analog to wetting on elastomers [20]. The contact line is implemented as a concentrated line force, leading to a Neumann balance with the substrate's surface tension that imposes the fold angle θ . The difference with [20] is the use of a poroelastic energy, with ψ given by the Gent model (cf. Supplemental Material [35]).

Numerical results for $\theta = 2\pi/3$ are presented in Fig. 3, which confirm the strong swelling near the fold tip. An increase of J is observed already at relatively large distance, confirming that the solution is fundamentally different from an incompressible fold. The swelling ratio J saturates due to strain stiffening, exactly at the values predicted by Eq. (11). Interestingly, an intermediate scaling law $J \sim r^{-\alpha}$ emerges in the “neo-Hookean limit” $I_{\max} \rightarrow \infty$. This scaling reflects the anticipated infinite-swelling paradox when strain stiffening is absent, which is confirmed by simulating the neo-Hookean model (blue solid line in Fig. 3). In this case, we numerically observe that stress and Finger tensors become isotropic in the vicinity of the tip. Admitting a divergent J in Eq. (5), an isotropic \mathbf{B} implies $\lambda \sim r^{1-1/b}$, predicting the observed exponent $\alpha = 2(1/b - 1)$ for the swelling ratio.

Implications for polymer networks.—Comparing creasing and wetting [Figs. 2(c) and 2(d)], we find a reversal of the solvent migration away from or toward the fold tip. What are the implications of these continuum singularities for experimental systems? For creasing, the singularity of pressure is relatively weak (logarithmic) and compressive

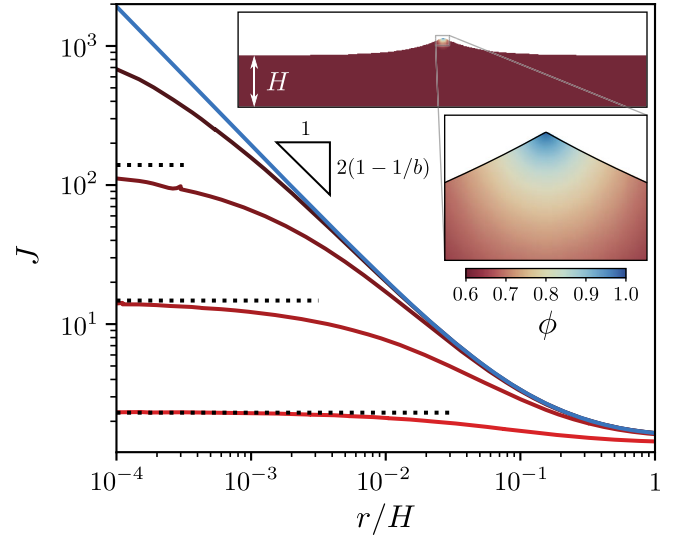


FIG. 3. Finite element simulation of a wetting ridge on a poroelastic substrate of thickness H . The swelling ratio J is plotted versus the radial distance to the fold tip, r/H , for the Gent model with $I_{\max} = 5, 32, 302, 3002$ (solid lines, red to black) and the neo-Hookean model ($I_{\max} = \infty$, blue solid line). Dashed lines are the saturations predicted by Eq. (11). Model parameters: $\chi = 0$, $Nv = 1$, $\theta = 120^\circ$ ($b = 2/3$), $\gamma/GH = 1$. Inset: full numerical domain and enlargement of the swollen tip.

in nature. In practice we estimate the value of the logarithm in Eq. (8) in the range 1–10, when, e.g., taking r to vary from molecular scales to the crease length r_0 (typically 100 μm). Depending on the material, such compressive stresses are typically uncritical. Thus, these deformations are expected to be reversible, corroborated by experiments showing the reversibility of creasing without material failure [43–45].

By contrast, the singularity of wetting requires further interpretation. The divergence of stress for a strain-stiffening model is much stronger (algebraic) and tensile in nature, and requires the polymers to become fully stretched near the fold tip. Even when considering a moderate range of r/r_0 , the predicted stress near the fold tip exceeds G by orders of magnitude. Thus we expect irreversible material failure close to the tip.

On hydrogels, such wetting-induced fracture has indeed been observed experimentally [26,27]. Local fracture at the fold tip, predicted from our analysis, thus offers an explanation for strong contact line pinning [46] observed on hydrogels [Fig. 4(a)]. Interestingly, however, wetting experiments on poroelastic crosslinked polydimethyl siloxane (PDMS), which is “swollen” by uncrosslinked polymer chains, do not exhibit any significant contact angle hysteresis—suggesting that pinning defects are absent. The key difference with hydrogels is the polymeric, i.e., macromolecular nature of the swelling fluid. This significantly reduces the mixing entropy as compared to hydrogels [$Nv \sim 1$ instead of $\sim 10^{-4}$; see Fig. 2(a)] and enables

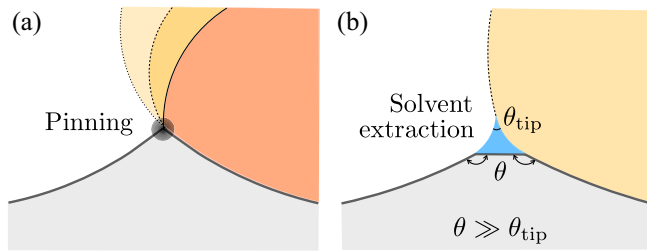


FIG. 4. Sketch of poroelastic wetting scenarios. (a) The stress singularity predicted by our theory can lead to a local, irreversible fracture of the polymer network. This can act as a site for contact line pinning (observed in hydrogels [46]). (b) Alternatively, the extraction of a liquid phase (observed for macromolecular solvents [23–25]) prevents sharp poroelastic folds and pinning due to irreversible damage is avoided.

the extraction of the fluid phase into a small meniscus with negative Laplace pressure. This scenario is sketched in Fig. 4(b): the formation of a sharp poroelastic fold is avoided by the extraction of solvent, which dramatically reduces the magnitude of stress. This effect has been observed experimentally in the context of adhesion [24] and wetting [23,25]. The precise conditions for solvent extraction remain to be identified, but clearly the geometric focussing of poroelastic stress plays a central role.

Outlook.—We have demonstrated that poroelastic folds generate intricate solvent distributions that are fundamentally different between wetting and creasing, and which are governed by nontrivial exponents. Our analysis offers an explanation for wetting-induced pinning and fracture, and opens a new route to poroelasticity under extreme deformations. While our analysis is restricted to equilibrium, it is clear that the divergence of stress will persist during transient diffusion of solvent. On shorter timescales, solvent depletion renders the crease tip a singular point, breaking the spatial invariance of the surface. This can cause pinning and hence might explain the annealable scars left behind by unfolded creases [29,43]. More generally, our findings show that the continuum framework of poroelasticity can break down near singular points, which must be addressed in future experiments or molecular simulations.

The authors thank J. Eggers for discussions. J. H. S. acknowledges financial support from NWO Vici (No. 680-47-632), and S. K. and J. H. S. acknowledge support from the University of Twente-Max Planck Center for Complex Fluid Dynamics, and funding from the German research foundation (DFG, Project No. KA4747/2-1). A. P. acknowledges startup funding from Syracuse University.

[1] P. J. Flory, *Principles of Polymer Chemistry* (Cornell University Press, Ithaca, 1953).

[2] G. T. Charras, J. C. Yarrow, M. A. Horton, L. Mahadevan, and T. Mitchison, Non-equilibration of hydrostatic pressure in blebbing cells, *Nature (London)* **435**, 365 (2005).

- [3] K. F. Cutting and R. J. White, Maceration of the skin and wound bed 1: Its nature and causes, *J. Wound Care* **11**, 275 (2002).
- [4] X.-F. Wei, E. Linde, and M. S. Hedenqvist, Plasticiser loss from plastic or rubber products through diffusion and evaporation, *npj Mater. Degrad.* **3**, 18 (2019).
- [5] L. R. Smith, S. Cho, and D. E. Discher, Stem cell differentiation is regulated by extracellular matrix mechanics, *Physiology* **33**, 16 (2018).
- [6] Y. Yang and M. W. Urban, Self-healing polymeric materials, *Chem. Soc. Rev.* **42**, 7446 (2013).
- [7] J. Dervaux and M. Ben Amar, Mechanical instabilities of gels, *Annu. Rev. Condens. Matter Phys.* **3**, 311 (2012).
- [8] V. Trujillo, J. Kim, and R. C. Hayward, Creasing instability of surface-attached hydrogels, *Soft Matter* **4**, 564 (2008).
- [9] T. Bertrand, J. Peixinho, S. Mukhopadhyay, and C. W. MacMinn, Dynamics of Swelling and Drying in a Spherical Gel, *Phys. Rev. Appl.* **6**, 064010 (2016).
- [10] B. Mota and S. Herculano-Houzel, Cortical folding scales universally with surface area and thickness, not number of neurons, *Science* **349**, 74 (2015).
- [11] T. Tallinen, J. Y. Chung, J. S. Biggins, and L. Mahadevan, Gyriification from constrained cortical expansion, *Proc. Natl. Acad. Sci. U.S.A.* **111**, 12667 (2014).
- [12] T. Tallinen, J. Y. Chung, F. Rousseau, N. Girard, J. Lefèvre, and L. Mahadevan, On the growth and form of cortical convolutions, *Nat. Phys.* **12**, 588 (2016).
- [13] J. Dervaux, Y. Couder, M.-A. Guedeau-Boudeville, and M. Ben Amar, Shape Transition in Artificial Tumors: From Smooth Buckles to Singular Creases, *Phys. Rev. Lett.* **107**, 018103 (2011).
- [14] S. J. Park, B. M. Weon, J. S. Lee, J. Lee, J. Kim, and J. H. Je, Visualization of asymmetric wetting ridges on soft solids with x-ray microscopy, *Nat. Commun.* **5**, 1 (2014).
- [15] E. R. Jerison, Y. Xu, L. A. Wilen, and E. R. Dufresne, Deformation of an Elastic Substrate by a Three-Phase Contact Line, *Phys. Rev. Lett.* **106**, 186103 (2011).
- [16] R. W. Style, R. Boltyskiy, Y. Che, J. S. Wettlaufer, L. A. Wilen, and E. R. Dufresne, Universal Deformation of Soft Substrates near a Contact Line and the Direct Measurement of Solid Surface Stresses, *Phys. Rev. Lett.* **110**, 066103 (2013).
- [17] B. Andreotti and J. H. Snoeijer, Statics and dynamics of soft wetting, *Annu. Rev. Fluid Mech.* **52**, 285 (2020).
- [18] R. W. Style, C. Hyland, R. Boltyskiy, J. S. Wettlaufer, and E. R. Dufresne, Surface tension and contact with soft elastic solids, *Nat. Commun.* **4**, 1 (2013).
- [19] A. Chakrabarti, A. Porat, E. Raphaël, T. Salez, and M. K. Chaudhury, Elastowetting of soft hydrogel spheres, *Langmuir* **34**, 3894 (2018).
- [20] A. Pandey, B. Andreotti, S. Karpitschka, G. J. van Zwieten, E. H. van Brummelen, and J. H. Snoeijer, Singular Nature of the Elastocapillary Ridge, *Phys. Rev. X* **10**, 031067 (2020).
- [21] M. Zhao, F. Lequeux, T. Narita, M. Roché, L. Limat, and J. Dervaux, Growth and relaxation of a ridge on a soft poroelastic substrate, *Soft Matter* **14**, 61 (2018).
- [22] Q. Liu and Z. Suo, Osmocapillary phase separation, *Extreme Mech. Lett.* **7**, 27 (2016).

- [23] Z. Cai, A. Skabeev, S. Morozova, and J. T. Pham, Fluid separation and network deformation in wetting of soft and swollen surfaces, *Commun. Mater.* **2**, 1 (2021).
- [24] K. E. Jensen, R. Sarfati, R. W. Style, R. Boltyanskiy, A. Chakrabarti, M. K. Chaudhury, and E. R. Dufresne, Wetting and phase separation in soft adhesion, *Proc. Natl. Acad. Sci. U.S.A.* **112**, 14490 (2015).
- [25] L. Hauer, Z. Cai, A. Skabeev, D. Vollmer, and J. T. Pham, Phase Separation in Wetting Ridges of Sliding Drops on Soft and Swollen Surfaces, *Phys. Rev. Lett.* **130**, 058205 (2023).
- [26] J. B. Bostwick and K. E. Daniels, Capillary fracture of soft gels, *Phys. Rev. E* **88**, 042410 (2013).
- [27] K. E. Daniels, S. Mukhopadhyay, P. J. Houseworth, and R. P. Behringer, Instabilities in Droplets Spreading on Gels, *Phys. Rev. Lett.* **99**, 124501 (2007).
- [28] M. van Gorcum, B. Andreotti, J. H. Snoeijer, and S. Karpitschka, Dynamic Solid Surface Tension Causes Droplet Pinning and Depinning, *Phys. Rev. Lett.* **121**, 208003 (2018).
- [29] M. A. J. van Limbeek, M. H. Essink, A. Pandey, J. H. Snoeijer, and S. Karpitschka, Pinning-Induced Folding-Unfolding Asymmetry in Adhesive Creases, *Phys. Rev. Lett.* **127**, 028001 (2021).
- [30] W. Hong, X. Zhao, J. Zhou, and Z. Suo, A theory of coupled diffusion and large deformation in polymeric gels, *J. Mech. Phys. Solids* **56**, 1779 (2008).
- [31] P. J. Flory, Thermodynamics of high polymer solutions, *J. Chem. Phys.* **10**, 51 (1942).
- [32] M. L. Huggins, Theory of solutions of high polymers¹, *J. Am. Chem. Soc.* **64**, 1712 (1942).
- [33] P. J. Flory and J. Rehner, Jr., Statistical mechanics of cross-linked polymer networks ii. Swelling, *J. Chem. Phys.* **11**, 521 (1943).
- [34] M. Singh and A. C. Pipkin, Note on Ericksen's problem, *Z. Angew. Math. Phys.* **16**, 706 (1965).
- [35] See Supplemental Material at <http://link.aps.org/supplemental/10.1103/PhysRevLett.130.228201>, which includes Refs. [36,37], for derivations of numerous expressions as used in the main text, and further details on the numerical simulations.
- [36] C. Henkel, M. Essink, G. Van Zwieten, E. Van Brummelen, U. Thiele, and J. Snoeijer, Soft wetting with (a) symmetric shuttleworth effect, *Proc. R. Soc. A* **478**, 20220132 (2022).
- [37] J. van Zwieten, G. van Zwieten, and W. Hoitinga, NUTILS 7.0 (2022), [10.5281/zenodo.6006701](https://doi.org/10.5281/zenodo.6006701).
- [38] The value of r_0 cannot be determined from the local corner analysis, but is inherited from matching to an outer geometry [29].
- [39] A. E. Green and W. Zerna, *Theoretical Elasticity* (Dover Publications, Inc., New York, 1992).
- [40] E. M. Arruda and M. C. Boyce, A three-dimensional constitutive model for the large stretch behavior of rubber elastic materials, *J. Mech. Phys. Solids* **41**, 389 (1993).
- [41] A. N. Gent, A new constitutive relation for rubber, *Rubber Chem. Technol.* **69**, 59 (1996).
- [42] C. O. Horgan, The remarkable Gent constitutive model for hyperelastic materials, *Int. J. Nonlinear Mech.* **68**, 9 (2015).
- [43] J. Yoon, J. Kim, and R. C. Hayward, Nucleation, growth, and hysteresis of surface creases on swelled polymer gels, *Soft Matter* **6**, 5807 (2010).
- [44] S. Cai, D. Chen, Z. Suo, and R. C. Hayward, Creasing instability of elastomer films, *Soft Matter* **8**, 1301 (2012).
- [45] D. Chen, S. Cai, Z. Suo, and R. C. Hayward, Surface Energy as a Barrier to Creasing of Elastomer Films: An Elastic Analogy to Classical Nucleation, *Phys. Rev. Lett.* **109**, 038001 (2012).
- [46] J. Y. Kim, S. Heyden, D. Gerber, N. Bain, E. R. Dufresne, and R. W. Style, Measuring Surface Tensions of Soft Solids with Huge Contact-Angle Hysteresis, *Phys. Rev. X* **11**, 031004 (2021).